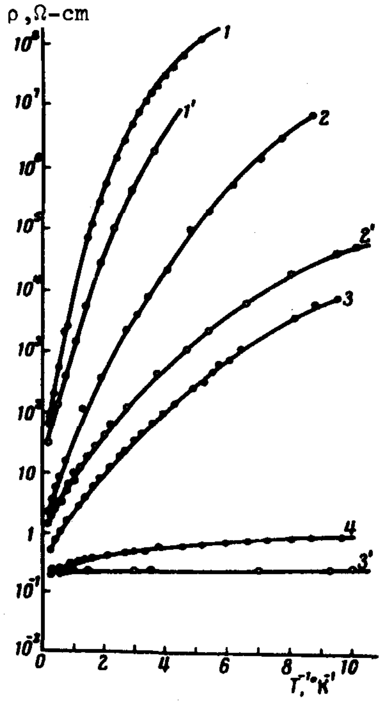

Fig. 2. The same plots as in Fig. 1 in a wider temperature range (down to 0.1°K).

metallic state into a state with $\varepsilon \neq 0$. Thus, the use of the second method resulted in a larger assortment of curves with the available samples.

Figure 2 shows the same plots of ρ against T^{-1} down to 0.1°K. It is seen from this figure that the activation energy of the impurity conductivity does not remain constant, but decreases continuously with decreasing temperature. For the weakly doped sample 1, the plot of the resistivity against the reciprocal temperature agrees well with the formula $\log \rho \sim T^{-1/4}$. With increasing concentration, the exponent increases, namely, $\log \rho \sim T^{-0.5}$ for sample 2 and $\log \rho \sim T^{-0.75}$ for sample 3. The fact that not all samples obeyed the $T^{-1/4}$ law predicted by Mott is not unexpected, since the conductivity of these samples is not described by the usual jump mechanism. It should be noted that the curves have a smooth form, starting with 4.2°K, so that the apparent linearity in the 4.2 - 1.3°K interval is due only to the narrowness of the temperature interval.

The investigation has thus shown that the impurity conductivity in doped germanium does not have a constant activation energy, and with decreasing temperature it is effected via states that come ever closer to the Fermi level.

The authors thank Professor S.M. Ryvkin, B.P. Zakharchenya, and B.I. Shklovskii for useful discussions of the results.

[1] N. Mott and W. Twose, Advances in Physics <u>10</u>, 107 (1961).
[2] N. Mott, Phil. Mag. <u>19</u>, 835 (1969).
[3] K. Lark-Horovitz, Semiconducting Materials, L. (1951).

EXPERIMENTAL INVESTIGATION OF TURBULENT PLASMA HEATING BY STRAIGHT-DISCHARGE SKIN CURRENT

L.E. Aranchuk, E.K. Zavoiskii, D.N. Lin, and L.I. Rudakov
Submitted 25 November 1971
ZhETF Pis. Red. 15, No. 1, 33 - 36 (5 January 1972)

The experiments were performed with the TN-5 Probkotron mirror machine [1, 2] under conditions when the plasma-heating current was strongly concentrated in the skin layer. In the experiments, the radius of the plasma column was 10 cm (the measured thickness of the skin layer was ∿3 cm, see below), and the length of the plasma column was 300 cm. The amplitude of the straight discharge current was 20 kA, with a period of 7.5 μsec and an initial voltage 40 kV. The containing magnetic field of the Probkotron was 5 kOe (8 kOe in the mirrors). The preliminary plasma density was $n_0 \geq 7 \times 10^{13}$ cm^{-3}, and the initial energy content was $n_0 T_0 \leq 2 \times 10^{14}$ eV-cm^{-3}.

The total discharge current was measured with a Rogowski loop placed outside the plasma. The current density distribution over the cross section of the plasma column was measured with a set of seven single-turn magnetic probes

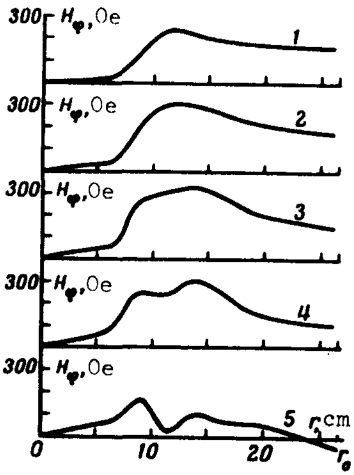

Fig. 1

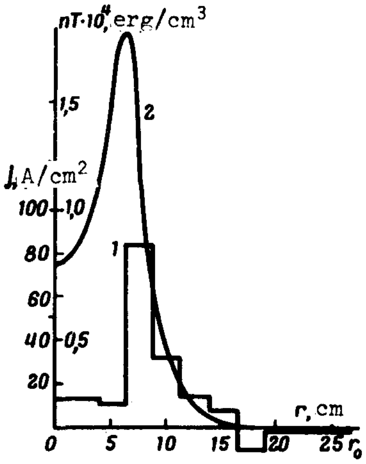

Fig. 2

Fig. 1. Radial distribution of azimuthal magnetic field at different instants of time (microseconds); 1 - 1.0, 2 - 1.5, 3 - 2.0, 4 - 2.5, 5 - 3.5.

Fig. 2. 1 - Distribution of current density at the instant 2.0 μsec, 2 - radial distribution of thermal energy $nT_\perp$ of the plasma at the instant 2.5 μsec.

disposed along the plasma radius in the central part of the setup. It is obvious that the distribution of the current density j_z over the plasma cross section can be calculated if the dependence of the current-induced magnetic field intensity H_ϕ on the distance r to the axis of the plasma column is known.

Figure 1 shows the radial distribution of the azimuthal magnetic field H_ϕ measured with the probes at different instants of the discharge. It is seen that during the first 3 microseconds of the discharge, when the turbulent heating commences, the magnetic field of the current hardly penetrates into the axial plasma region with radius ∿6 cm. During this time interval, the distribution of the magnetic field H_ϕ is stable, thus indicating macroscopic stability of the plasma column.

Figure 2 (curve 1) shows the distribution of the current density j_z over the cross section at 2.0 μsec after the start of the discharge (the total discharge current at this instant is 18 kA). We see that the bulk of the current flows in a narrow surface layer that does not extend beyond the outer boundary of the preliminary plasma. The measurements show that the current skin-layer thickness δ is equal to ∿3 cm when the radius of the current-carrying plasma column is $r_{pl} \simeq 10$ cm. Knowing the thickness of the skin layer, we can calculate the conductivity of the plasma and the effective collision frequency ν_{eff} in the skin layer, using the formula $\delta^2 = c^2/4\pi\sigma\omega = c^2\nu_{eff}/\omega\omega_{pe}$, where ω is the oscillation frequency of the straight-discharge current. From this we get $\nu_{eff} = 10^9$ sec^{-1}.

If the anomalous conductivity of the plasma is the consequence of ion-acoustic instability, which limits the current density to the level $en(T_e/M)^{1/2}$, the formula for δ can also be written in the form $\delta \simeq c/\omega_{pi}[H^2/8\pi nT]^{-1/2}$ [3]. In our experiments, the skin layer calculated from this formula amounts to

2.4 cm, which agrees with the measured value of δ. An analogous result was obtained in [4].

The distribution of the plasma pressure $P_\perp = nT_\perp$ over the cross section of the plasma columns at different instants of the discharge was determined by measuring the distributions of the fields H_ϕ and H_z. In the case of axial symmetry, as in these experiments, nT at equilibrium is given by the relation

$$\frac{\partial nT_\perp}{\partial r} = -\frac{1}{4\pi}\left[\frac{H_\phi}{r}\frac{\partial}{\partial r}(rH_\phi) + H_z\frac{\partial H_z}{\partial r}\right].$$

The distribution $H_z(r)$ at different instants of time was obtained with the aid of the same system of magnetic probe as used for the measurement of $H_\phi(r)$.

Figure 2 (curve 2) shows the nT(r) distribution in the central part of the chamber at 2.5 μsec after the start of the discharge. Comparison of curves 1 and 2 of Fig. 2 shows that even though the current density is large only in the thin skin layer, the plasma is effectively heated over the entire cross section of the column. Figure 2 shows also that in the case of turbulent heating the energy released in the plasma stays practically in the volume occupied by the preliminary plasma.

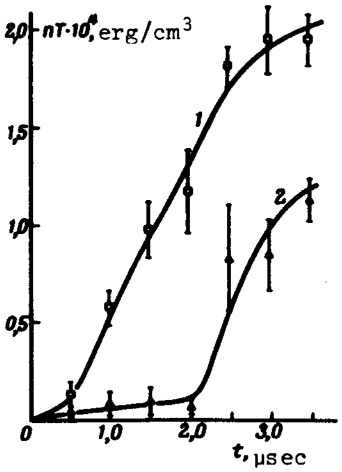

Fig. 3. Time dependence of $nT_\perp$: 1 - in the skin layer, 2 - on the axis of the plasma column.

Control experiments have shown that the appearance of hot plasma in the axial part of the column cannot be attributed to the influx of heat from the electrode regions along the magnetic field.

Figure 3 shows plots of the growth of the energy content of the plasma in the skin layer and on the axis of the column. According to these curves, the plasma-heating delay time in the axial region is approximately 1.5 μsec, i.e., the speed of heat propagation across the magnetic field towards the center of the chamber is unusually high. It reaches 5×10^6 cm/sec.

Experiment thus shows that an initially bounded plasma column practically does not expand during the heating time, but the heat is transported with high speed from the skin layer to the interior of the plasma.

It should be stated in conclusion that the peculiarity we observed in the turbulent heating offers a promise of greatly decreasing the total current needed to heat plasma in large thermonuclear installations, by concentrating the current in the skin layer.

[1] E.K. Zavoiskii, S.L. Nedoseev, L.I. Rudakov, V.D. Rusanov, and S.D. Fanchenko, Plasma Physics and Controlled Thermonuclear Reactions, Vol. II, p. 679, Vienna, 1969.
[2] L.E. Aranchuk and S.L. Nedoseev, Zh. Eksp. Teor. Fiz. 61, 1856 (1971) [Sov. Phys.-JETP 34, No. 5 (1972)].
[3] B.N. Breizman, N.V. Mirnov, and D.D. Ryutov, Zh. Tekh. Fiz. 39, 1817 (1969) [Sov. Phys.-Tech. Phys. 14, 1365 (1970)].
[4] L.V. Dubovoi, V.P. Fedyakov, and V.P. Fedyakova, Zh. Eksp. Teor. Fiz. 59, 1475 (1970) [Sov. Phys.-JETP 32, 805 (1971)].